J. Phys. C: Solid State Phys. **19** (1986) 963–974. Printed in Great Britain

Intrinsic and magnetic impurity induced ^{19}F nuclear magnetic relaxation in the superionic conductor $K_{0.4}Bi_{0.6}F_{2.2}$

J P Donoso†, L N Oliveira†, H Panepucci†, A Cassanho‡ and H Guggenheim‡§

† Departamento de Física e Ciência dos Materiais, Instituto de Física e Química de São Carlos, Universidade de São Paulo, 13560, São Carlos, S.P., Brazil

‡ Instituto de Pesquisas Energéticas e Nucleares (IPEN), Caixa Postal 11049, 01000, São Paulo, S.P., Brazil

§ Bell Laboratories, Murray Hill, New Jersey 07974, USA

Received 12 November 1984, in final form 31 July 1985

Abstract. Measurements of the ^{19}F nuclear relaxation times T_1 and T_2 are reported for the fluorite-structured $K_{0.4}Bi_{0.6}F_{2.2}$ single crystal, pure and doped with Fe^{3+}, as a function of temperature. We examine in some detail the problem of the asymmetric T_1 minimum in the nominally pure sample and we propose a basic approach that, from the experimental data, allows us to determine both the spectral density and the correlation function. The effect of magnetic impurity on the relaxation process and the defect formation energy in these fluorite systems are discussed.

1. Introduction

The study of crystals with the fluorite structure that exhibit unusually high anion conductivities well below their melting temperatures is receiving considerable attention, motivated by their potential importance in connection with application to high energy density storage systems and the physics associated with liquid-like transport in solids (Boyce and Huberman 1979, Salamon 1979, Chandra 1981). In particular, the ternary compounds with fluorite structure have a much higher ionic conductivity at room temperature than the binary compounds, such as PbF_2, due to the built-in defect structure (Cassanho *et al* 1983). Many studies, including x-ray crystallography (Matar *et al* 1980), neutron diffraction (Soubeyroux *et al* 1982), differential thermal analysis (Cassanho *et al* 1983), ionic diffusion and conductivity measurements (Réau *et al* 1978, Cassanho *et al* 1983, Shafer and Chandrashekhar 1981) have been made on these materials.

In a previous paper (Donoso *et al* 1983) we reported the measurements of the ^{19}F nuclear relaxation time T_1 and T_2 for the fluorite-structured $K_{0.36}Bi_{0.64}F_{2.22}$, as a function of temperature and frequency. The salient feature of our results was the presence of a broad minimum and a highly asymmetric shape in the $\ln T_1$ versus T^{-1} curve; we suggested that this could be a characteristic of highly disordered systems. The crystals are strongly disordered on a microscopic scale because of local charge compensation since the cation sites in the fluorite structure are randomly occupied by the ions K^+ and Bi^{3+}.

That charge compensation influences the diffusion of the ^{19}F ions is suggested by the

temperature dependence of the longitudinal relaxation times for the ternary fluorite $K_{0.4}Bi_{0.6}F_{2.2}$, which differs qualitatively from the data reported for binary fluorites (Boyce and Huberman 1979). Unfortunately this difference renders the traditionally applied phenomenological Bloembergen–Purcell–Pound (Bloembergen *et al* 1948) formulation and more elaborate microscopic approaches, such as those of Wolf (1974), Wolf *et al* (1977) and Figueroa *et al* (1979) (see also Chang *et al* (1981) and references in Boyce and Huberman (1979)), which describe remarkably well the temperature and orientation dependence of T_1 in BaF_2, unapplicable to the present case. At low T in particular, the $T_1(T)$ curves reported here and in previous works (Cassanho *et al* 1983, Donoso *et al* 1983) disagree strikingly even with the more accurate, first-principles calculation, so asymmetrical are they.

In the present paper we investigate phenomenologically the question of the skew T_1 minimum. This frequently encountered feature of $\ln T_1$ versus T^{-1} plots has been the subject of a recent theoretical study (Albano *et al* 1983, 1984). Instead of following the analysis of Albano *et al*, who hypothesise a distribution of correlation times defining the Bloembergen–Purcell–Pound (BPP) assumed exponential decay of the spin-correlation function, we prefer to use a single correlation time combined with a non-exponential, general function $f(t/\tau)$. This turns out to be a more basic approach, which introduces no adjustable parameters and, as shown in § 3, allows us to determine both the spectral density and the correlation function f. Essential to the procedure is the existence of a single correlation time and hence a single relaxation mechanism. This condition, which turns out to be an advantage allowing us to distinguish the dipolar coupling from extrinsic sources of relaxation, constitutes the foundation of the iterative procedure developed by Halstead *et al* (1982) to determine the spectral density. We believe that the approach used here is easier to apply and less subject to uncertainties due to experimental errors.

We also discuss the effect of magnetic impurity on the relaxation process in this fluorite system and, finally, we comment briefly on the defect formation energy for these materials. A preliminary report of this work appeared in the proceedings of the Conference on 'Defects in Insulating Crystals' (August 1984).

2. Experimental details

$K_{0.4}Bi_{0.6}F_{2.2}$ single crystals were grown from the melt by the horizontal zone technique and the Bridgman method (Cassanho *et al* 1983). ^{19}F T_1 and T_2 measurements were carried out with a pulsed NMR spectrometer operating at 23 MHz. T_1 was determined using the progressive saturation method above room temperature. The multiple-pulse saturation recovery method was used below room temperature, i.e. for $T_1 \gg T_2$. The saturation recovery method was also used in the region of the T_1 minimum. For T_2, spin-echo techniques were used. The shortest spin–spin relaxation times were obtained directly from the free induction decay of the magnetisation following a $\pi/2$ pulse. The high temperature probe and furnace are described elsewhere (Donoso *et al* 1983).

The effects of magnetic impurities were investigated in samples obtained from a single-crystal rod, zone-refined during the growth process and sectioned afterwards. The samples were encapsulated in sealed quartz tubes, that were heated at 300 °C for 20 min to test for possible contamination and after that, slowly cooled. This resulted in samples with very low (sample S1) to high (sample S3) concentrations of impurity ions. The lattice constant, as obtained by Guinier–Häag diffractometry, was 5.914 ± 0.003 Å in all the three samples. It was observed by Matar *et al* (1980) that the fluorite structured

solid solution $K_{1-x}Bi_xF_{2x+1}$ ($0.5 \leqslant x \leqslant 0.7$) obeys Vegard's law; according to their data our compound should be $K_{0.4}Bi_{0.6}F_{2.2}$. X-ray fluorescence measurements indicated that the impurity was iron, but the accuracy of the fluorescence measurements is not sufficient to determine the Fe concentration accurately. The analysis showed a progressive decrease of Fe^{3+} in the 5–15 ppm concentration range. The T_2 and T_1 relaxation times are shown in figures 1 and 2 respectively as a function of reciprocal temperature. For the

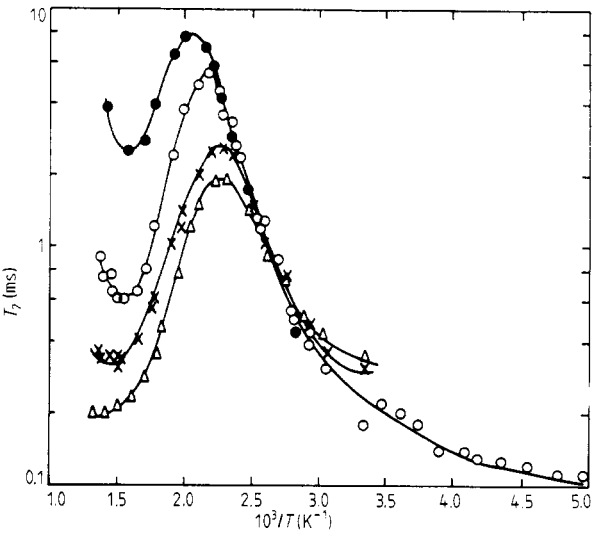

Figure 1. Spin–spin relaxation time (T_2) of ^{19}F as a function of reciprocal temperature in $K_{0.4}Bi_{0.6}F_{2.2}$, pure (at the Larmor frequency of 23.6 MHz) (●) and doped with Fe^{3+} (at the Larmor frequency of 23 MHz): (○, S1; ×, S2; △, S3). The full curves are a guide to the eye.

sake of comparison the results for a nominally pure sample measured at 23.6 MHz, from Donoso *et al* (1983), are also included. Unfortunately the composition of this nominally pure sample is significantly different from the other three samples and does not permit the comparison of activation behaviours. According to Matar *et al* (1980), the activation energy changes linearly with the composition; this behaviour characterises the activation extracted from our T_1 data at high temperatures. The purpose of the comparison here presented is to emphasise the remarkable asymmetry of the T_1 minimum in the nominally pure sample.

The effects of temperature cycling as the experiment is being run were investigated on another nominally pure sample not previously heated. The relaxation time measurements were made when both increasing and decreasing the temperature. The results are shown in figure 3 as a function of reciprocal temperature, from room temperature to 600 °C. Independently, measurements were made after quenching a fresh sample, obtained from the same boule, by heating at 500 °C for 30 min and then cooling it quickly. The lattice constant of these samples, also obtained by Guinier–Hägg diffractometry, was $a = 5.907 \pm 0.003$ Å. Accordingly, the compound can be written as $K_{0.39}Bi_{0.61}F_{2.22}$. We present results for this sample, whose composition is somewhat different from the nominally pure sample in figures 1 and 2 to show that the striking asymmetry in the T_1 curves is characteristic of an entire class of compounds. X-ray fluorescence analysis shows

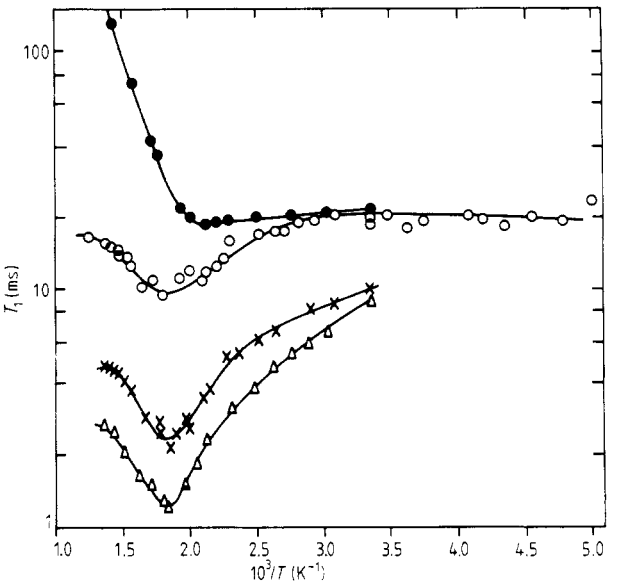

Figure 2. Spin–lattice relaxation time (T_1) of ^{19}F as a function of reciprocal temperature in $K_{0.4}Bi_{0.6}F_{2.2}$, pure (at the Larmor frequency of 23.6 MHz) (●) and doped with Fe^{3+} (at the Larmor frequency of 23 MHz): (○, S1; ×, S2; △, S3). The full curves are a guide to the eye.

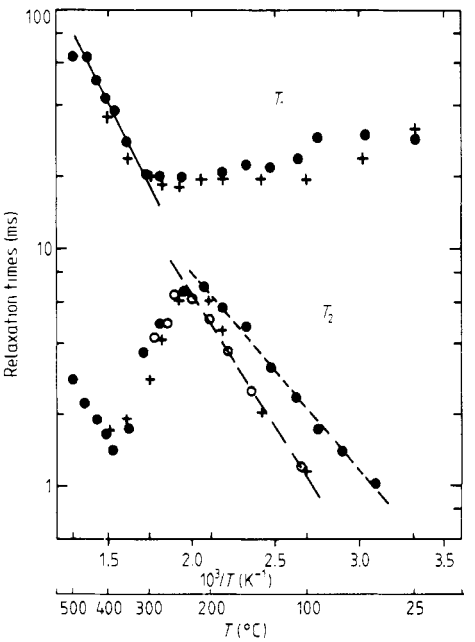

Figure 3. NMR relaxation times of ^{19}F as a function of reciprocal temperature in $K_{0.36}Bi_{0.64}F_{2.22}$ nominally pure, at the Larmor frequency of 23 MHz. The measurements were made increasing (●) and decreasing (+) the temperature. By fitting the T_1 data (full curve) we obtained an activation energy of 0.28 eV. The T_2 data yield 0.17 eV (for increasing T) and 0.3 eV (for decreasing T). Data from a second run increasing T in the same, but annealed, sample are shown by (○) and yield an activation energy of 0.23 eV.

the unavoidable paramagnetic impurity (Fe^{3+}) to be present, at very low concentration levels, in this sample also.

3. Results and discussion

The main features of our experimental results are as follows: (i) the presence of a minimum of T_2, dependent on magnetic impurity concentration, in the high temperature region (figure 1); (ii) the presence of a broad minimum and a highly asymmetric shape in the ln T_1 versus T^{-1} curve for the pure sample (figures 2 and 3); (iii) a saturation of the relaxation rates, due to the high impurity levels, in the high temperature region (figure 2); (iv) the presence of different slopes in the ln T_2 versus T^{-1} curve for measurements made in the heating or in the cooling parts of the temperature cycle (figure 3).

Experimental results for the temperature dependence of NMR rates in solids are often interpreted on the basis of the BPP hopping model, which, assuming an average residence time for the ion, attributes an exponential time dependence, $e^{-t/\tau}$, for the nuclear spin correlation function. For a discussion of this model, the reader is referred to Boyce and Huberman (1979), who observe that the relaxation rates T_1^{-1} and T_2^{-1} are related to the spectral densities $J^{(q)}(\omega)$ according to

$$\left.\begin{aligned} T_1^{-1} &= \tfrac{3}{2}\alpha[J^{(1)}(\omega_0) + J^{(2)}(2\omega_0)] \\ T_2^{-1} &= \tfrac{3}{8}\alpha[J^{(0)}(0) + 10J^{(1)}(\omega_0) + J^{(2)}(2\omega_0)] \end{aligned}\right\} \tag{1}$$

where $\alpha = \gamma^4 h^2 I(I+1)$, γ is the gyromagnetic ratio, I the nuclear spin and $\omega_0 = \gamma H_0$ is the Larmor precession frequency in the magnetic field H_0; the spectral densities $J^{(q)}(\omega)$ are proportional to the Fourier transform of the spin correlation function and, in the BPP model, are given by

$$J^{(q)}(\omega) = C_q \frac{\tau}{1 + (\omega\tau)^2} \tag{2a}$$

where the constants C_q are in the proportion

$$C_0 : C_1 : C_2 = 6:1:4. \tag{2b}$$

Assuming an Arrhenius temperature dependence for the hopping time τ:

$$\tau = \tau_0 \exp(U/k_B T) \tag{3}$$

where τ_0 is the inverse of the attempt frequency, U is an activation energy, and k_B the Boltzmann constant, one expects a symmetrical V-shaped curve for the logarithmic plot of T_1 as a function of the inverse temperature, i.e. ln T_1 should have a minimum as a function of $1/T$ with slopes on either side that are numerically identical and give the activation energy U.

Inspection of figures 2 and 3 shows, however, that the model applies to neither the pure nor the doped samples. In fact, all curves display clearly asymmetrical minima for T_1 as a function of $1/T$, a behaviour qualitatively similar to that reported for Na–β-alumina (Walstedt *et al* 1977) which may be accounted for by assuming a gaussian distribution of activation energies. More recently, on the basis of a technique first introduced to evaluate the dipole correlation function in the case of translational diffu-

sion, Bjorkstam and Villa (1980) calculated the 2D-diffusional correlation function in Na–β-alumina and proposed phenomenological rules to determine activation energies.

In this paper, to explain the T_1 asymmetries we introduce an alternative, in our view more fundamental, approach. We replace the BPP-assumed exponential time dependence for the spin correlation function by an unknown function $f(t/\tau)$. In § 3.1.1 we show that (*a*) this procedure is consistent with the Larmor frequency dependence of the experimental results for the pure sample, and (*b*) the correlation function $f(t/\tau)$ may be derived from the measured relaxation rates. Section 3.1.2 discusses the T_1 results for the doped samples and shows that the insight gained in this analysis allows qualitative interpretation of the experimental data.

3.1. Results for T_1

3.1.1. Pure samples. In a pure sample one expects that the spin correlation function depends only on the hopping of the ^{19}F ions and that it scales with the hopping time τ, i.e. is of the form $f(t/\tau)$. The spectral densities are proportional to the Fourier transform of the correlation function (cf equations (2*a*) and (2*b*)):

$$J^{(q)}(\omega) = C_q \int_{-\infty}^{+\infty} f(t/\tau) \exp(i\omega t)\, dt \tag{4}$$

and therefore can be written

$$J^{(q)}(\omega) = C_q \tau \int_{-\infty}^{+\infty} f(z) \exp(i\Omega z)\, dz \tag{5}$$

where $\Omega = \omega\tau$ and the integration variable is now the dimensionless scale $z = t/\tau$. It then follows from equation (1) that

$$T_1^{-1} \sim \tau\left\{\int_{-\infty}^{+\infty} f(z)[C_1 \exp(i\Omega z) + C_2 \exp(2i\Omega z)]\, dz\right\}. \tag{6}$$

For given $f(z)$, the product $T_1\tau$ depends only on the dimensionless parameter $\Omega = \omega_0\tau$. Since the temperature dependence of T_1 is determined at different Larmor frequencies, this conclusion and hence its premise—that the correlation function depends on a single relaxation time—can be tested. We will come back to this point while discussing figure 4.

Before that, however, we consider equation (6) in the limits of large and of small Ω, to show that it determines the asymptotic forms $J^{(q)}(\omega \to \infty)$ and $J^{(q)}(\omega \to 0)$ for the spectral density.

(i) $\Omega \ll 1$. Since it is expected that $f(z) \to 0$, for $z \gg 1$, the integral of the right-hand side of equation (6) is only significant for $\Omega z \ll 1$. It follows that

$$T_1^{-1} \sim (C_1 + C_2)\tau \int_{-\infty}^{+\infty} f(z)\, dz \qquad (\Omega \ll 1) \tag{7}$$

which, for convenience, we write

$$T_1^{-1} \sim \tau \int_{-\infty}^{+\infty} f(z) \exp(i\Omega z)\, dz \qquad (\Omega \ll 1). \tag{8}$$

(ii) $\Omega \gg 1$. Because of the complex exponentials on the right-hand side of equation (6), the dominant contribution to the integral comes from the range $0 < z < \Omega^{-1} \ll 1$. To a good approximation one can therefore write

$$T_1^{-1} \sim \tau C_1 \int_{-\infty}^{+\infty} f(z=0)\exp(i\Omega z)\,dz + \tau C_2 \int_{-\infty}^{+\infty} f(z=0)\exp(2i\Omega z)\,dz. \tag{9}$$

Changing the integration variable in the second integral on the right-hand side from z to $z/2$, we then have

$$T_1^{-1} \sim \tau C_1 \int_{-\infty}^{+\infty} f(z=0)\exp(i\Omega z)\,dz + \tfrac{1}{2}\tau C_2 \int_{-\infty}^{+\infty} f(z=0)\exp(i\Omega z)\,dz$$

or

$$T_1^{-1} \sim \tau(C_1 + \tfrac{1}{2}C_2) \int_{-\infty}^{+\infty} f(z=0)\exp(i\Omega z)\,dz. \tag{10}$$

At this point, however, we again note that the dominant contribution to the integrals come from the range $0 < z < \Omega^{-1} \ll 1$, which allows us to write

$$T_1^{-1} \sim \tau \int_{-\infty}^{+\infty} f(z)\exp(i\Omega z)\,dz. \tag{11}$$

Compared with equation (5), equations (8) and (11) show that, in the limits $\Omega \ll 1$ and $\Omega \gg 1$, respectively, the product $(T_1\tau)^{-1}$ is the spectral density $J^{(q)}(\Omega)$ divided by the hopping time τ. Figure 4 applies this result to the T_1 data for the nominally pure sample (Donoso *et al* 1983). In order to plot $(T_1)^{-1}$ as a function of $\omega_0\tau$ we first need the hopping activation energy; from the motional narrowing region (400 K > T > 300 K) of the Arrhenius plot of $T_2(T)$, shown in figure 1, we determine U = 4000 K. Next, we arbitrarily choose the temperature T_0 = (4000/2.1) K and the Larmor frequency $\bar{\omega}$ = 23.6 MHz. At T_0 the hopping time $\bar{\tau}$ equals $\tau_0 e^{U/T_0}$, so that the ratio $\bar{\tau}/T_1\tau$ is independent of τ_0 and can be readily computed from the $T_1(T)$ data. Likewise, the ratio $\omega_0\tau/\bar{\omega}\tau_0$, independent of τ_0, can be easily evaluated for any given Larmor frequency ω_0 and temperature T. Within the experimental error, the di-logarithmic plots of $\bar{\tau}/T_1\tau$ as a function of $\omega_0\tau/\bar{\omega}\tau_0$ for three Larmor frequencies reported in Donoso *et al* (1983) yield the same curve.

This universal behaviour, which confirms the scaling assumption underlying equation (6) and indicates that the dipolar interaction governs the relaxation in the nominally pure sample, deserves a brief discussion. Equation (6) hinges on the assumption that a single correlation time τ controls the relaxation; the construction of figure 4 hinges on the premise that $\tau = \tau_0 \exp(U/k_BT)$. Therefore, were there two or more competing correlation times, or were there a single correlation time with different activation energies in different temperature ranges, the agreement between the open circles, filled circles, and crosses in the figure would be spoiled. One could conceive, for instance, that paramagnetic impurities account for the relatively fast longitudinal relaxation for T < 400 K. Were this the case, however, two different energies, associated with electron spin relaxation and with ionic hopping, would control the correlation time for T < 400 K and T > 400 K, respectively. If, for example, the former were U' = 0.2 eV while the latter were U = 0.34 eV (the energy applied to the construction of figure 4), in the low temperature range the open circles in figure 4 would be displaced horizontally by 0.22 K^{-1} relative to the crosses, a sizeable shift that would spoil the agreement between the three sets of data. What is more, the temperature dependence of electron spin relaxation often follows a power law (see, e.g. Miller and Mahendroo 1968, Tse and Lowe 1968) in contrast with the Arrhenius construction of figure 4; were this the case, the agreement would be even worse. Paramagnetic impurities can, of course, dominate the longitudinal relaxation at much lower temperatures, as in the study of Ce-doped CaF_2 by Tse and Lowe (1968). In

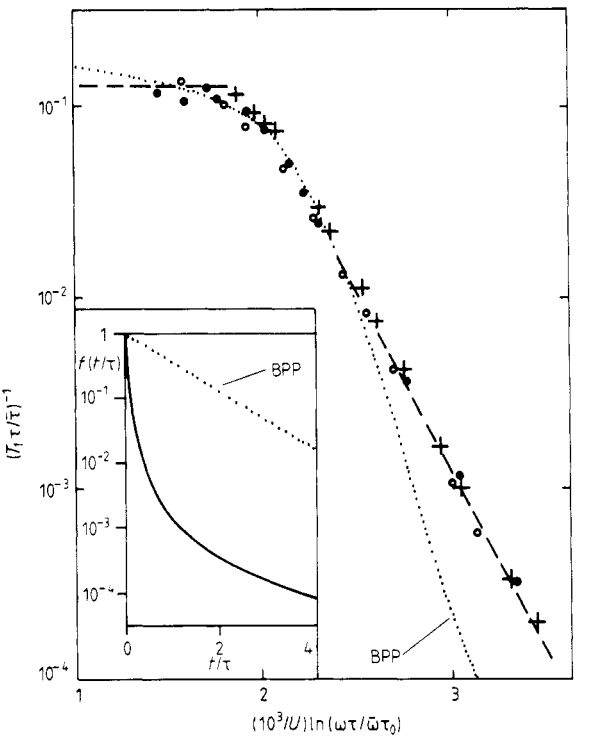

Figure 4. Graphical procedure showing that for the pure sample T_1 scales with the ^{19}F hopping time and determining the spectral density J as a function of the Larmor frequency. On the logarithmic scale vertical axis is the inverse of the product $T_1\tau$ normalised by the (arbitrary) parameter $\bar{\tau}$, defined in § 3.1.1; the horizontal axis is the product $\omega\tau$ divided by $\bar{\omega}\tau_0$, $\bar{\omega}$ being the arbitrarily chosen Larmor frequency 23.6 MHz, and τ_0 the inverse attempt frequency: $U = 0.34$ eV. That T_1^{-1} scales with τ (and hence results from dipolar relaxation) is shown by the universal curve describing, within experimental errors, data collected at the three Larmor frequencies: (○) 10.5 MHz, (●) 23.6 MHz, (+) 35.8 MHz. As discussed in the text, the asymptotic least-square fits to this curve, shown as a broken curve yields equation (13) for the spectral density and produce the inset spin correlation function $f(t/\tau)$. For comparison, both the main plot and the inset show as dotted curves the corresponding BPP expression, equation (2*a*), best fitting the T_1 data for a nominally pure sample at high temperature ($T > 550$ K) in figure 2.

the temperature range covered by our measurements, however, the congruence in figure 4 shows that a single mechanism—the dipolar interaction—with a single activation energy ($U = 0.34$ eV) dominates the relaxation.

In addition, the accord among the three sets of points in figure 4 determines the asymptotic spectral densities. Since, in the asymptotic limits, $J^{(q)}(\omega) \sim T_1^{-1}$ (cf equations (5), (8) and (11)), the least-square fits shown as broken curves in figure 4 yield the following asymptotic expressions for the spectral densities in the limits of large and of small frequencies:

$$\left.\begin{aligned} J^{(q)}(\omega) &\sim \tau & \omega &\ll 1/\tau \\ J^{(q)}(\omega) &\sim \tau(\omega\tau)^{-1.06} & \omega &\gg 1/\tau. \end{aligned}\right\} \tag{12}$$

It follows from comparing equation (12) with equation (2) that, at high frequencies, the spectral density for the $K_{1-x}Bi_xF_{2x+1}$ system is considerably larger than the

BPP prediction. This large spectral density enhances the relaxation rates at low temperatures, where $\omega_0\tau \gg 1$, and is responsible for the asymmetry of the curve for our nominally pure sample in figure 2. In the high temperature limit (i.e. $\omega_0\tau \ll 1$), in contrast, equations (12) and (2) become identical so that, as the curve for the pure sample in figure 2 shows, T_1 follows the Arrhenius temperature dependence expected in the BPP model.

From the asymptotic limits for the spectral density an approximation to the spin correlation function may be obtained. To this end we combine equations (12) in a single expression approaching the asymptotic forms in the limits of large and small $\omega\tau$:

$$J^{(q)}(\omega) = \frac{C\tau}{1 + (\omega\tau)^{1.06}} \tag{13}$$

where C is an (unknown) constant. The correlation function $f(t/\tau)$, equal to the Fourier transform of $J^{(q)}(\omega)$, may now be evaluated numerically, the constant C being determined by the condition $f(t = 0) = 1$. The resulting plot of f as a function of time is shown in the inset of figure 4 compared with the BPP assumed exponential decay of the correlation function. The rapid, nearly logarithmic drop in $f(t/\tau)$ at short times is in sharp contrast with the uniform decay of the exponential function. The origin of this feature, which is responsible for the relatively large spectral density at $\omega\tau \gg 1$, remains unclear to us and will be the subject of a more detailed microscopic study of this fluorite system.

3.1.2. Doped samples. The interaction with magnetic impurities introduces characteristic time scales affecting the ^{19}F relaxation and hence, in the case of doped samples, invalidates the scaling argument developed in § 3.1.1. In particular, as first discussed in the work of Vernon *et al* (1981), the hyperfine interaction with the impurities is most effective in relaxing the spin of the NN ^{19}F nuclei for hopping rates τ^{-1} that are comparable with the (Larmor) frequency $\gamma A_{\alpha z}/\hbar$ associated with the off-diagonal terms A_{xz}, A_{yz} of the hyperfine tensor. The sharp dips (i.e. maxima of the relaxation rates) in the plots for samples S1–S3 in figure 2, reducing T_1 in rough proportion to impurity concentration, suggest that the condition

$$\tau^{-1} = \gamma A \alpha z/\hbar \tag{14}$$

is satisfied at the temperature $T \simeq 550$ K.

Depending on whether (i) $\tau^{-1} \ll \gamma A_{\alpha z}/\hbar$, (ii) $\tau^{-1} \approx \gamma A_{\alpha z}/\hbar$ or (iii) $\tau^{-1} \gg \gamma A_{\alpha z}/\hbar$ one can therefore divide figure 2 into three temperature ranges:

(i) $T < 400$ K. In this low temperature range, due to the long residence times, the interaction with the magnetic impurities is a relatively ineffective source of relaxation. In particular, for the case of the lowest impurity concentration, (S1 in figure 2) the relaxation times then approach the constant found in the pure sample. As discussed in § 3.1.1, this constant is associated with the slow decay of the spectral density at high Larmor frequencies. For larger concentration (S2 and S3 in figure 2) the relaxation due to the magnetic impurities is added to this dipolar relaxation and, hence, progressively reduces the spin–lattice relaxation times.

(ii) $400\ \text{K} < T < 700\ \text{K}$. In this intermediate temperature range, the hyperfine interaction with the magnetic impurities is the dominant source of relaxation and reduces the relaxation time in proportion (Vernon 1981) to impurity concentration. Since the nominally pure sample contains a low unavoidable concentration of magnetic

impurities, one might expect a minimum at $T \simeq 550$ K for the T_1 data represented by the filled circles in figure 2. In view of the relatively low level of concentration (estimated at 1 ppm), however, this minimum is masked by the asymmetric, broad dipole-interaction minimum at $T \simeq 500$ K.

(iii) $T > 700$ K. At high temperatures, as the hopping rate τ^{-1} approaches the electronic Larmor frequency for the magnetic impurities, the fast motion of the ^{19}F nuclei generates a microwave frequency hyperfine field capable of flipping the electronic spin. As first pointed out by Vernon *et al* (1981) and Vernon and Jaccarino (1982), the resulting rapidly fluctuating impurity magnetic moment then becomes an important source of nuclear spin relaxation, in the present case responsible for the barely discernible levelling of the T_1 curves at the highest temperatures shown in figure 2.

3.2. Results for T_2

In the BPP model, as a result of motional narrowing, T_2 steadily increases as a function of the inverse temperature. A similar behaviour is expected for the spectral density depicted in figure 4, which, as mentioned in § 3.1, in the limit of low frequencies agrees with the BPP spectral density, equation (2). Contrasting with the results for T_1 this feature makes T_2 sensitive to very low impurity levels, and hence, in the following discussion, warrants no formal distinction between nominally pure (but with inevitable impurities) and doped samples.

In support of these considerations, the results for the pure sample in figure 1 display the qualitative features found in the data for the doped samples. Motional narrowing is apparent at 50 °C, and for $T < 400$ K, T_2 follows the Arrhenius law with an activation energy $E_a \simeq 0.35$ eV, being hence proportional to the ^{19}F hopping time τ. Above $T = 450$ K, the hyperfine interaction with the magnetic impurity spin becomes the dominant source of relaxation, so that T_2 decreases reaching a minimum when the hopping frequency $\nu = \tau^{-1}$ becomes equal to the diagonal component, Azz, of the hyperfine tensor (Vernon *et al* 1981, Vernon and Jaccarino 1982).

In the region of motional narrowing, as expected, T_2 is independent of the impurity concentration c. For $T > 450$ K, however, in agreement with the results reported by Vernon *et al* (1981), the relaxation rates increase in rough proportion to the values $c = 1$–2, 5, 9 and 15 ppm found for the pure sample and samples S1, S2 and S3 respectively.

3.3. Activation energies

As mentioned in § 2, in the low temperature region, T_2 depends on whether the sample is heated for the first time or cooled (figure 3) as the experiment is being run. Such distinct behaviours are not observed in conductivity measurements because the samples must be previously heated in their holders in order to provide good contact between the sample and the electrodes and after that, slowly cooled. Since (1) our results obtained in the heating part of the cycle agree with those obtained on a quenched sample and (2) relaxation times measured for an annealed sample and in the cooling part of the cycle likewise agree, one is lead to associate two activation energies with the hopping of the F-ions. More specifically one expects that, in order to hop, a F-ion must (*a*) overcome an energy barrier, and (*b*) sit next to a vacancy. In an annealed sample each of these two conditions will be associated with a different energy: the barrier height ΔE_b and the defect formation energy ΔE_d, respectively, so that the

hopping time is determined by an activation energy $\Delta E = \Delta E_b + \Delta E_d$. In a quenched sample, in contrast, even at the lowest temperatures, a large number of defects will be present. In this case, one expects that the barrier height, ΔE_b, and the hopping activation energy, ΔE_q, be identical.

In the cooling part of the cycle shown in figure 3, defects initially present in the samples are progressively eliminated as the temperature is slowly decreased from a maximum of approximately 600 °C. This is an annealing procedure, following which the T_2 data yield an activation energy

$$\Delta E_a = \Delta E_b + \Delta E_d \simeq 0.3\,\text{eV}. \tag{15}$$

In contrast, when a fresh sample (where its growth results in a large number of built-in defects), is heated, the less pronounced increase of T_2 with the temperature is associated with a smaller activation energy:

$$\Delta E_q = \Delta E_b \simeq 0.17\,\text{eV}. \tag{16}$$

From equations (15) and (16), one can produce an estimate of $\Delta E_d \simeq 0.13$ eV for the defect formation energy.

The T_1 data show, in the top part of figure 3, essentially the same curve in the heating and in the cooling parts of the temperature cycle. This result ratifies the analysis carried out in § 3.1, according to which at low temperature the spectral density $J^{(q)}(\omega)$ is nearly independent of τ. Equation (12) shows that for $\omega\tau \gg 1$

$$J^{(q)}(\omega) \sim \omega^{-1.06}\tau^{-0.06} \qquad (\omega\tau \gg 1). \tag{17}$$

If the weak τ-dependence contained in equation (17) is neglected, one expects that T_1 be independent of the activation energies. At high temperatures, on the other hand, the large number of thermally activated defects effaces all distinction between quenched and annealed samples.

4. Conclusions

In this paper we report measurements of the longitudinal and transverse relaxation times for the ^{19}F nuclei in the fluorite structured superionic conductor $K_{0.4}Bi_{0.6}F_{2.2}$. Pure samples and samples doped with three different concentrations of Fe^{3+} were studied as a function of temperature.

The most prominent feature of the results is a marked asymmetry of the minimum in the Arrhenius plot of T_1 for the nominally pure sample. Through the graphical procedure illustrated in figure 4, we were able to trace the origin of this asymmetry to a fast, nearly logarithmic decay of the spin correlation function for times that are short in the scale of the ionic hopping rate. Having determined the spin correlation function and the associated spectral density, we were subsequently able to present a qualitative discussion of the results for the doped samples, showing that at high temperatures the interaction with the magnetic impurities is responsible for the measured relaxation rates.

Essential to the discussion of the experimental results was the scaling argument presented in § 3.1.1, which allowed us to distinguish intrinsic (i.e. associated with the dipole interaction) from extrinsic features due to the interaction with the magnetic impurities. Moreover, by producing the graphical procedure in figure 4 and hence

allowing us to determine the spin correlation function, the argument provides a potentially important starting point for a microscopic theory of the kinetics of ionic transport in the superionic conductors here considered.

While the development of such a theory lies beyond the scope of the present paper, the apparent conflict between the theoretical analysis presented here and in our previous preliminary report (Donoso *et al* 1983) calls for a brief discussion, aimed at reconciling the two approaches. In this earlier publication, for three different Larmor frequencies, fits to the asymmetrical ln T_1 versus T^{-1} curves resulted from assuming that the ionic hopping time τ was governed by a distribution of activation energies (Walstedt *et al* 1977). Although mathematically different from the time scaling approach introduced here, the hypothesis of a distribution of barrier heights is qualitatively equivalent to the non-exponential correlation function in the inset of figure 4; for, in the scale of the average hopping frequency, those hopping events associated with the low energy tail of the distribution will rapidly take place and hence quickly reduce spin correlation. At subsequent times, the decay of the correlation function depends on the hopping of ions trapped by the barriers on the high energy side of the distribution and is, therefore, much slower. The argument, which suggests that the distribution of activation energies is one of a variety of possible explanations for the asymmetric T_1 minima, emphasises the need for a microscopic understanding of ionic transport in $K_{1-x}Bi_xF_{2x+1}$ and other systems, such as Na–β-alumina, in which similar features have been found.

Acknowledgments

The financial support of CNPq and FINEP (Brazil) are gratefully acknowledged.

References

Albano A M, Beckmann P A, Carrington M E, Fisch E E, Fusco F A, O'Neill A E and Scott M E 1984 *Phys. Rev.* **30** 2334
Albano A M, Beckmann P A, Carrington M E, Fusco F A, O'Neill A E and Scott M E 1983 *J. Phys. C: Solid State Phys.* **16** L979
Bjorkstam J L and Villa M 1980 *Phys. Rev.* B **22** 5025
Bloembergen N, Purcell E M and Pound R V 1948 *Phys. Rev.* **73** 679
Boyce J B and Huberman B A 1979 *Phys. Rep.* **51** 189–265
Cassanho A, Guggenheim H and Walstedt R E 1983 *Phys. Rev.* B **27** 6587
Chandra S 1981 *Superionic Solids* (Amsterdam: North-Holland)
Chang H, Engelsberg M and Lowe I J 1981 *Solid State Ionics* **5** 609
Donoso J P, Panepucci H, Cassanho A and Guggenheim H 1983 *Solid State Commun.* **48** 95–7
Figueroa D R, Strange J H and Wolf D 1979 *Phys. Rev.* B **19** 148
Halstead T K, Metcalfe K and Jones T C 1982 *J. Magn. Res.* **47** 292
Matar S, Réau J M, Lucat C, Grannec J and Hagenmuller P 1980 *Mater. Res. Bull.* **15** 1295
Miller J R and Mahendroo P P 1968 *Phys. Rev.* **174** 369
Réau J M, Portier J, Levasseur A, Villeneuve G and Pouchard M 1978 *Mater. Res. Bull.* **13** 1415
Salamon M B (ed.) 1979 *Physics of Superionic Conductors* (Berlin: Springer-Verlag)
Shafer M W and Chandrashekhar G B 1981 *Solid State Ionics* **5** 629
Soubeyroux J L, Réau J M, Matar S, Villeneuve G and Hagenmuller P 1982 *Solid State Ionics* **6** 103
Tse D and Lowe I J 1968 *Phys. Rev.* **166** 292
Vernon S P and Jaccarino V 1982 *Phys. Rev.* B **26** 6077
Vernon S P, Thayamballi P, Hogg R D, Hone D and Jaccarino V 1981 *Phys. Rev.* B **24** 3756
Walstedt R E, Dupree R, Remeika J P and Rodrigues A 1977 *Phys. Rev.* B **15** 3442
Wolf D 1974 *Phys. Rev.* B **10** 2710
Wolf D, Figueroa D R and Strange J H 1977 *Phys. Rev.* B **15** 2545